LETTER

https://doi.org/10.1038/s41586-018-0546-8

A natural variant and engineered mutation in a GPCR promote DEET resistance in *C. elegans*

Emily J. Dennis[1], May Dobosiewicz[2], Xin Jin[2,6], Laura B. Duvall[1], Philip S. Hartman[3], Cornelia I. Bargmann[2,4] & Leslie B. Vosshall[1,4,5]*

DEET (*N,N*-diethyl-*meta*-toluamide) is a synthetic chemical identified by the US Department of Agriculture in 1946 in a screen for repellents to protect soldiers from mosquito-borne diseases[1,2]. Since its discovery, DEET has become the world's most widely used arthropod repellent and is effective against invertebrates separated by millions of years of evolution—including biting flies[3], honeybees[4], ticks[5], and land leeches[3]. In insects, DEET acts on the olfactory system[5–12] and requires the olfactory receptor co-receptor *Orco*[7,9–12], but exactly how it works remains controversial[13]. Here we show that the nematode *Caenorhabditis elegans* is sensitive to DEET and use this genetically tractable animal to study the mechanism of action of this chemical. We found that DEET is not a volatile repellent, but instead interferes selectively with chemotaxis to a variety of attractant and repellent molecules. In a forward genetic screen for DEET-resistant worms, we identified a gene that encodes a single G protein-coupled receptor, *str-217*, which is expressed in a single pair of chemosensory neurons that are responsive to DEET, called ADL neurons. Mis-expression of *str-217* in another chemosensory neuron conferred responses to DEET. Engineered *str-217* mutants, and a wild isolate of *C. elegans* that carries a *str-217* deletion, are resistant to DEET. We found that DEET can interfere with behaviour by inducing an increase in average pause length during locomotion, and show that this increase in pausing requires both *str-217* and ADL neurons. Finally, we demonstrated that ADL neurons are activated by DEET and that optogenetic activation of ADL neurons increased average pause length. This is consistent with the 'confusant' hypothesis, which proposes that DEET is not a simple repellent but that it instead modulates multiple olfactory pathways to scramble behavioural responses[10,11]. Our results suggest a consistent motif in the effectiveness of DEET across widely divergent taxa: an effect on multiple chemosensory neurons that disrupts the pairing between odorant stimulus and behavioural response.

We explored whether and how *C. elegans* nematodes respond to DEET during chemotaxis[14,15] (Fig. 1a) and tested three competing hypotheses for the mechanism of DEET: 'smell-and-repel', which states that the olfactory detection of DEET triggers avoidance[8,12]; 'masking', which proposes that DEET blocks olfactory pathways that mediate attraction[6,7]; and 'confusant', which states that DEET modulates multiple olfactory sensory neurons to scramble the perception of an otherwise attractive stimulus[10,11].

We first tested the smell-and-repel hypothesis. DEET alone was not repellent when presented to *C. elegans* as a volatile point source (Fig. 1b)—similar to results from *Drosophila melanogaster* flies[7], *Apis mellifera* bees[4], and *Aedes aegypti* mosquitoes[11], but in contrast to results from *Culex quinquefasciatus* mosquitoes[8]. To investigate whether DEET masks responses to attractive odorants[6,7] or directly inhibits their volatility[8], we presented DEET alongside the attractant isoamyl alcohol and found that DEET had no effect on attraction (Fig. 1c). In considering alternative ways to present DEET, we mixed low concentrations of DEET uniformly into chemotaxis agar (Fig. 1d). DEET–agar reduced chemotaxis to isoamyl alcohol in a dose-dependent manner (Fig. 1e). We tested three additional attractants—butanone, diacetyl and pyrazine—and the volatile repellent 2-nonanone. DEET decreased attraction to butanone and avoidance of 2-nonanone, indicating that DEET affects responses to both positive and negative chemosensory stimuli (Fig. 1f). DEET also affected chemotaxis to diacetyl, but not to pyrazine (Fig. 1f). Notably, both diacetyl and pyrazine are sensed by the AWA sensory neuron. This is similar to *D. melanogaster*, in which DEET can disrupt responses to some odorants—and not others—even in a single chemosensory neuron[10].

In *D. melanogaster* and *A. aegypti*, DEET inhibits attraction to complex natural odour blends[7,11]. In *C. elegans*, DEET eliminated chemotaxis to the food odour of OP50 *Escherischia coli* bacteria (Fig. 1g). Supplementing bacterial odour with pyrazine, but not isoamyl alcohol, restored chemotaxis (Fig. 1g). To exclude the possibility that pyrazine is able to overcome the effect of DEET because of a higher effective concentration, we carried out dose–response experiments with isoamyl alcohol (Fig. 1h) and pyrazine (Fig. 1i), and found that at all tested concentrations, DEET interfered with isoamyl alcohol chemotaxis but not with pyrazine chemotaxis. DEET chemosensory interference is therefore odour-selective, and affects responses to both attractive and repellent stimuli.

Previous work to identify the genetic basis of sensitivity to DEET using forward genetics has yielded both an X-linked DEET-insensitive *D. melanogaster* mutant[16] and a dominant genetic basis for insensitivity to DEET in mosquitoes[17], but neither study identified the underlying genes. Reverse genetic experiments in *D. melanogaster* and three mosquito species have shown that *orco* is required for sensitivity to DEET[7,9–12], but this gene is insect-specific[18]—which raises the question of which pathways are used in non-insect invertebrates. We therefore carried out a forward genetic screen for *C. elegans* mutants capable of chemotaxing towards isoamyl alcohol on DEET–agar plates (Fig. 2a). Of five DEET-resistant worms, three produced offspring that chemotaxed towards isoamyl alcohol on DEET–agar plates (Fig. 2b). We used whole-genome sequencing to identify candidate mutations in two strains, and focused on *LBV003*—this maps to *str-217*, which encodes a predicted G protein-coupled receptor (Fig. 2c, d). Over the course of mapping *str-217*, we discovered that a divergent strain of *C. elegans* isolated in Hawaii (CB4856 (Hawaiian)) is naturally resistant to DEET (Fig. 2e) and contains a deletion in *str-217* (*str-217*^{HW}) that leads to a predicted frame shift and early stop codon (Fig. 2c, d, Supplementary Data). This is not a unique phenomenon: 119 out of 247 sequenced strains in the *C. elegans* Natural Diversity Resource[19] contained predicted changes in STR-217, compared to the N2 wild type (Supplementary Data). We next tested three near-isogenic lines with a single, homozygous genomic segment of Hawaiian chromosome V introgressed into a wild-type background[20] (Fig. 2e). Only the ewIR74 line contains *str-217*^{HW} and was resistant to DEET (Fig. 2e). Expressing a rescue–reporter strain (Fig. 2f) in *LBV003* (Fig. 2g) or *ewIR74* (Fig. 2h) rendered both strains fully sensitive to DEET (Fig. 2g, h).

[1]Laboratory of Neurogenetics and Behaviour, The Rockefeller University, New York, NY, USA. [2]Lulu and Anthony Wang Laboratory of Neural Circuits and Behaviour, The Rockefeller University, New York, NY, USA. [3]Department of Biology, Texas Christian University, Fort Worth, TX, USA. [4]Kavli Neural Systems Institute, New York, NY, USA. [5]Howard Hughes Medical Institute, New York, NY, USA. [6]Present address: Society of Fellows, Harvard University, Cambridge, MA, USA. *e-mail: Leslie.Vosshall@rockefeller.edu

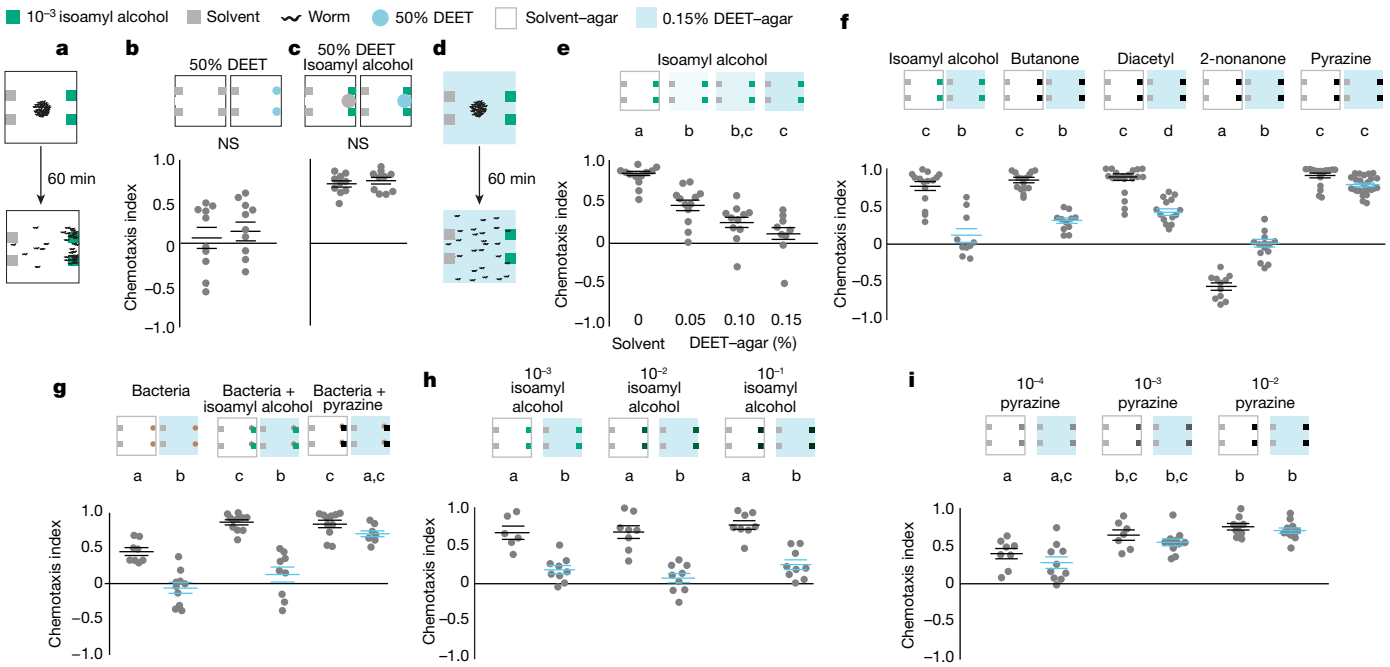

Fig. 1 | DEET interferes with chemotaxis in wild-type *C. elegans*. **a**, Schematic of chemotaxis assay. **b**, **c**, Chemotaxis with point-source stimuli of DEET without (**b**) or with (**c**) isoamyl alcohol. **d**, Chemotaxis assay on DEET–agar plates. **e**, Chemotaxis to isoamyl alcohol with different concentrations of DEET in the agar. **f**, Chemotaxis to indicated odorants. **g**, Chemotaxis to bacterial food source with indicated odorants. **h**, **i**, Chemotaxis dose–response to isoamyl alcohol (**h**) and pyrazine (**i**). In **b**, **c**, and **e**–**i**, each dot represents a chemotaxis index of a single population assay. Schematics indicate experimental conditions in the corresponding column in the plot, according to the key provided at the top of the figure (except where indicated otherwise, the key applies to all figures). In a given panel, data labelled with different letters are significantly different from each other; mean ± s.e.m. (horizontal blue or black lines on plots), $P < 0.05$, two-sided *t*-test (**b**, **c**) or one-way (**e**) or two-way (**f**–**i**) ANOVA and Tukey's post hoc test. NS, not significant. See Supplementary Data for sample sizes and details of statistical analyses.

In insects, DEET interacts with chemosensory neurons[7,9–12]. We used calcium imaging to investigate whether DEET modulates the primary sensory neurons (AWC neurons) required for the detection of isoamyl alcohol[21]. AWC neurons responded to the addition of DEET with a rapid increase in calcium that decreased to baseline over the course of 11 min of chronic DEET stimulation (Fig. 3a). In the presence of DEET, the responses of AWC neurons to isoamyl alcohol decreased in magnitude, but there were no significant differences in AWC-neuron activity between wild type and *str-217*$^{-/-}$, a predicted null mutant produced by CRISPR–Cas9 genome editing (Fig. 3a–c). The polymodal nociceptive neurons, named ASH, also responded to DEET (Fig. 3d, e), but worms that lack ASH neurons are fully DEET-sensitive (Fig. 3f). This suggests that DEET resistance requires additional neurons.

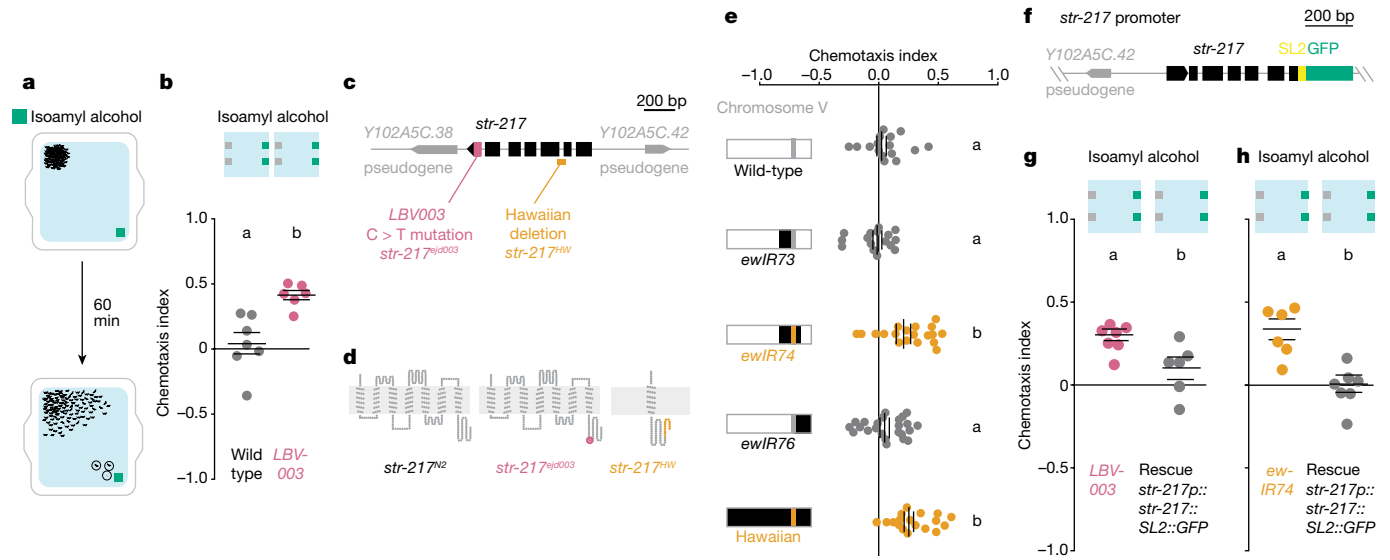

Fig. 2 | *str-217* mutants are resistant to DEET. **a**, Schematic of forward genetic screen with DEET-resistant mutants circled. **b**, Chemotaxis of indicated strains. **c**, Genomic locus of *str-217*. **d**, STR-217 protein snake plots in indicated strains. **e**, Schematic of chromosome V (left), and chemotaxis (right) in indicated strains. **f**, *str-217* rescue–reporter construct. **g**, **h**, Chemotaxis of indicated strains. In **b**, **e**, **g**, **h**, each dot represents a chemotaxis index of a single population assay. In a given panel, data labelled with different letters are significantly different from each other; mean ± s.e.m., $P < 0.05$, ANOVA and Tukey's post hoc test (**e**) and two-sided *t*-test (**b**, **g**, **h**). See Supplementary Data for sample sizes and details of statistical analyses.

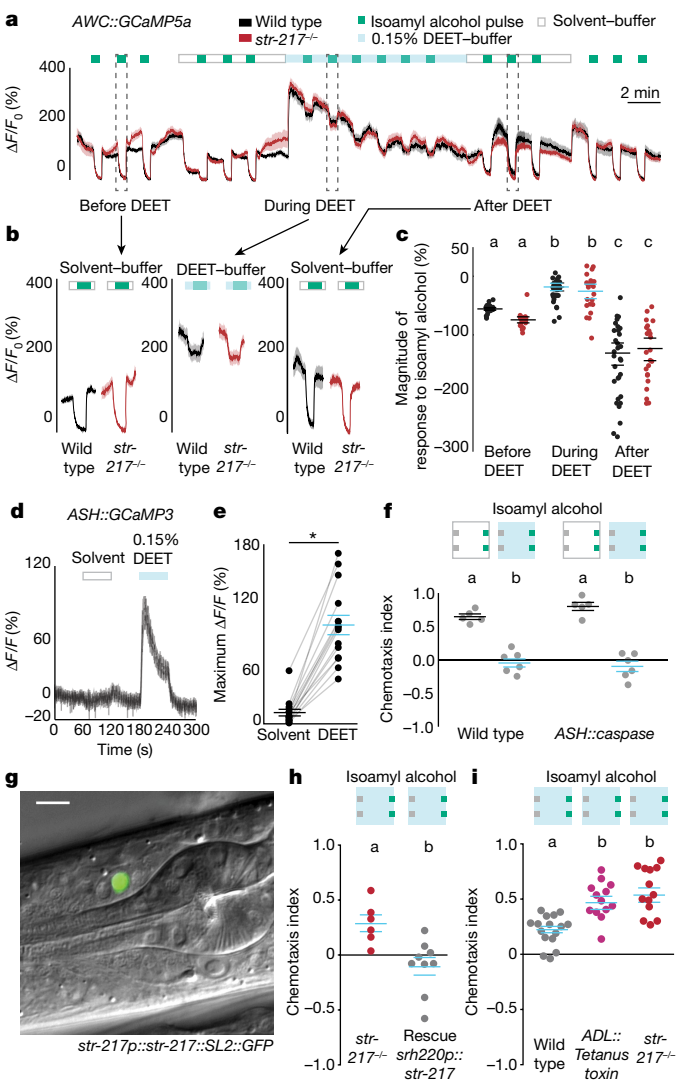

Fig. 3 | Several *C. elegans* neurons respond to DEET but ADL neurons are required for sensitivity to DEET. a, Average traces of GCaMP activity in AWC^{ON} cells of indicated genotype over a 36-min experiment. **b**, A subset of traces from **a**, re-plotted separately. **c**, Response magnitudes of data shown in **b**. **d**, GCaMP activity in ASH neurons to indicated stimuli. **e**, Quantification of **d**. **f**, Chemotaxis of indicated strains to isoamyl alcohol. **g**, *str-217* rescue–reporter GFP expression in a single ADL neuron. Scale bar, 10 μm. **h**, **i**, Isoamyl alcohol chemotaxis of indicated strains. In **a**, **b**, **d**, each trace represents mean (dark line) ± s.e.m. (lighter area) GCaMP response of all worms of each genotype. In **c**, **e**, each dot represents the response of a single worm. In **f**, **h**, **i**, each dot represents a chemotaxis index of a single population assay. In a given panel, data labelled with different letters are significantly different from each other; mean ± s.e.m., $P < 0.05$, two-way (**b**, **e**) or one-way (**h**) ANOVA with Tukey's post hoc test, or paired *t*-test (**d**, **g**). In **e**, $^*P < 0.05$. See Supplementary Data for sample sizes and details of statistical analyses.

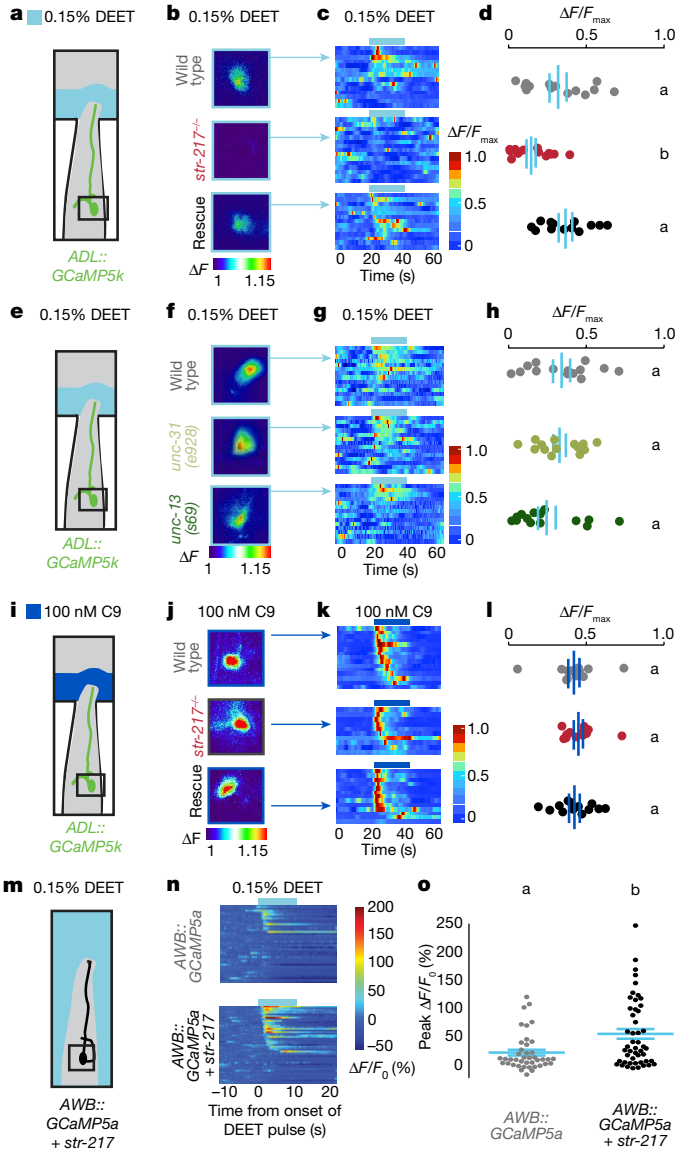

Fig. 4 | *str-217* is necessary for ADL responses to DEET and can confer DEET sensitivity to AWB neurons. a, **e**, **i**, **m**, Schematics of calcium imaging. **b**, **f**, **j**, Pseudo-coloured images of ADL neurons responding to 0.15% DEET (**b**, **f**) or 100 nM C9 (**j**) in worms of indicated genotype (fold increase in mean fluorescence 20 s during first stimulus pulse/mean of 20 s before the stimulus pulse). Arrows point to corresponding worm in subsequent panels. **c**, **g**, **k**, Heat maps of GCaMP activity in response to DEET (**c**, **g**) or C9 (**k**). Each row represents activity in one worm. **d**, **h**, **l**, Mean normalized responses of the data in **c**, **g**, **k** during entire pulse of DEET (**d**, **h**) or C9 (**l**). **n**, Heat maps of AWB-neuron calcium imaging response to 0.15% DEET; each row represents imaging from one worm cropped to show the 10-s before, during, and after the DEET pulse. **o**, Quantification of **n**. In **d**, **h**, **l**, **o**, each dot represents a single neuron in a single worm. In a given panel, data labelled with different letters are significantly different from each other; mean ± s.e.m. $P < 0.05$, one-way ANOVA and Tukey's post hoc test (**d**, **h**, **l**) or two-sided *t*-test (**o**). The rescue construct in **c** is the same as that shown in Fig. 3g, h. See Supplementary Data for sample sizes and details of statistical analyses.

To identify such neurons, we determined where *str-217* is expressed by examining our *str-217* rescue–reporter strain; we found GFP expression in a single pair of ADL chemosensory neurons (Fig. 3g). This was unexpected because ADL neurons are not required for chemotaxis to isoamyl alcohol[22], which suggests an indirect role in DEET chemosensory interference. To confirm that *str-217* expression in ADL neurons is required for DEET sensitivity, we expressed *str-217* in ADL neurons in *str-217*$^{-/-}$ mutants using a different ADL promoter, *srh-220p*. Expressing *str-217* in ADL neurons rendered this mutant sensitive to DEET (Fig. 3h). To investigate whether ADL neurons are required for DEET sensitivity, we inhibited chemical synaptic transmission by expressing the tetanus toxin light chain in ADL neurons[23,24]. These worms showed similar DEET resistance to that of *str-217* mutants (Fig. 3i), which demonstrates that ADL neurons contribute to DEET sensitivity.

Because both *str-217* and ADL neurons contribute to DEET sensitivity, we used calcium imaging to investigate whether ADL neurons respond to DEET and whether this requires *str-217* (Fig. 4a). Wild type and *str-217*$^{-/-}$ mutants that carry a rescue plasmid—but not *str-217*$^{-/-}$ mutants—showed calcium responses to DEET in ADL neurons,

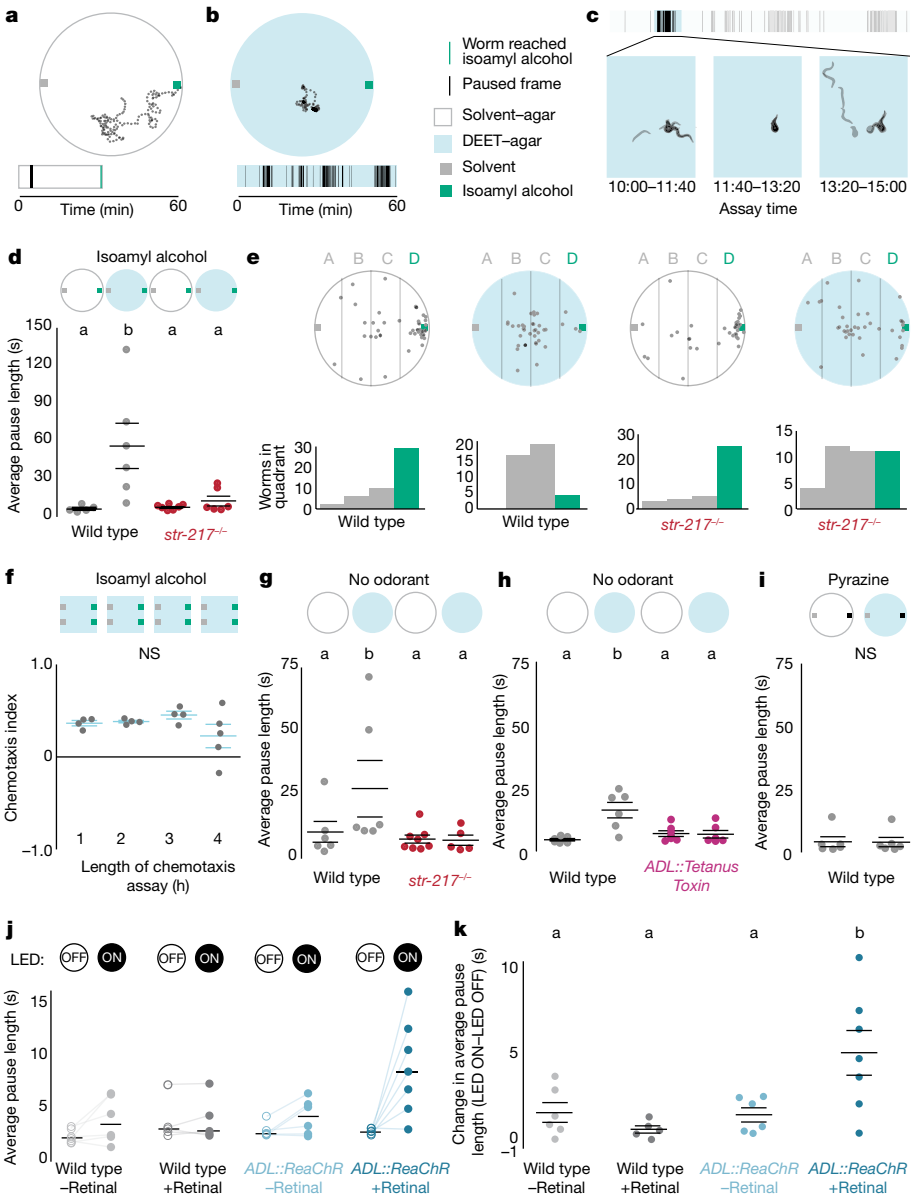

Fig. 5 | DEET increases average pause length by activating *str-217* and ADL neurons. a, **b**, Top, example trajectories of a single wild-type worm chemotaxing to isoamyl alcohol on solvent–agar (**a**) or DEET–agar (**b**). Each dot depicts the *x*, *y* position every 10 s. Bottom, raster plots of paused frames for the worm shown above. **c**, Example pauses from **b**. Images were extracted and converted to silhouettes every 6 s and superimposed. **d**, Average pause length of indicated stimuli and genotypes. **e**, Top, location of worms in **d** after 60 min. Bottom, histograms of worm locations. **f**, Wild-type chemotaxis on DEET at indicated times. **g**, **i**, Average pause length of indicated stimuli and genotypes. **j**, Average pause length of indicated genotypes and LED status (off or on). Lines connect experimental pairs. **k**, Difference in average pause length for each experimental pair in **j**. In **d**, **f**–**k**, each dot represents a single experimental plate. In a given panel, data labelled with different letters are significantly different from each other; mean ± s.e.m. $P < 0.05$, one-way (**f**) or two-way (**d**, **g**–**k**) ANOVA and Tukey's post hoc test. See Supplementary Data for sample sizes and details of statistical analyses.

albeit with some variability in the response (Fig. 4a–d). To exclude the possibility that DEET activates ADL neurons indirectly, we measured calcium responses in ADL neurons in *unc-13* and *unc-31* mutants, which are deficient in synaptic vesicle fusion[25] and dense-core vesicle fusion[26], respectively. ADL-neuron responses to DEET were normal in both strains (Fig. 4e–h). A known agonist of ADL neurons—the pheromone C9[23]—activated ADL neurons in wild-type, *str-217*$^{-/-}$ mutant and rescued worms (Fig. 4i–l), which suggests that the lack of DEET responsiveness in *str-217* is selective.

We then investigated whether *str-217* is sufficient to confer DEET responses in vitro in HEK293T cells or in vivo in AWB olfactory sensory neurons, which respond only weakly to DEET. Although DEET did not activate HEK293T cells that express *str-217* (Supplementary Data), in vivo mis-expression of *str-217* in AWB neurons significantly increased the sensitivity to DEET of these sensory neurons (Fig. 4m–o). This suggests that *str-217* either encodes a DEET receptor or cooperates with other proteins to increase sensitivity to DEET.

We next tracked the position and posture of individual worms on DEET–agar or solvent–agar plates (Fig. 5a–c). Wild-type worms, but not *str-217*$^{-/-}$ mutants (Fig. 5d), showed marked increases in average pause length on DEET–agar. Although *str-217*$^{-/-}$ mutants are resistant to DEET compared to wild type, their chemotaxis is not fully resistant to DEET (Fig. 3h) and many *str-217*$^{-/-}$ worms never reached the odorant source (Fig. 5e). Additionally, prolonging the assays did not significantly increase performance in wild-type worms (Fig. 5f). We suspect that DEET has additional effects on chemotaxis in addition to increasing pause duration.

To test whether the increase in pausing on DEET occurs only during chemotaxis, we tracked wild-type, *str-217*$^{-/-}$ mutant (Fig. 5g), and *ADL::Tetanus toxin* (Fig. 5h) worms on DEET–agar and solvent–agar

plates without odorants. *ADL::Tetanus toxin* worms express an inhibitor of evoked synaptic vesicle release in ADL neurons. Of these, only wild-type worms had an average pause length that was longer on DEET–agar than on solvent–agar (Fig. 5g, h), and this was not seen during pyrazine chemotaxis (Fig. 5i).

To test whether ADL activity alone is sufficient to increase average pause length, we optogenetically activated the light-sensitive ion channel ReaChR[27] in ADL neurons in wild-type worms and observed an increase in average pause length (Fig. 5j, k). We conclude that ADL neurons mediate the increase in average pause length seen on DEET–agar, and speculate that the increase in long pauses is one mechanism by which DEET interferes with chemotaxis.

Here we add the nematode *C. elegans* to known DEET-sensitive animals and uncover a neuronal mechanism for DEET-induced behaviour. This work opens up *C. elegans* as a system to test new repellents in vivo and to discover additional genes and neurons that respond to DEET. The molecular mechanism by which the *str-217* mutation renders ADL neurons insensitive to DEET and worms resistant to DEET remains to be understood. *str-217* encodes an orphan G protein-coupled receptor that is evolutionarily unrelated to DEET-sensitive insect odorant receptors. Our results are consistent with the hypothesis that *str-217* is a DEET receptor or the hypothesis that it interacts with additional proteins to make ADL neurons sensitive to DEET. Pyrazine chemotaxis is not disrupted by DEET, consistent with our model in which DEET is not a simple repellent but is instead a modulator of behaviour that interferes with chemotaxis to some—but not all—odorants. The *str-217*-dependent mechanism of action of DEET in nematodes is reminiscent of the 'confusant' hypothesis in insects, in which DEET alters responses of individual olfactory sensory neurons to attractive odorants[7,10], thereby interfering with behavioural attraction. In *C. elegans*, DEET inhibits attraction to some odorants by activating neurons that induce competing behaviours, such as pausing. We speculate that the promiscuity of DEET in interacting with multiple molecules and chemosensory neurons across vast evolutionary scales is the key to the broad effectiveness of this chemical.

Online content

Any methods, additional references, Nature Research reporting summaries, source data, statements of data availability and associated accession codes are available at https://doi.org/10.1038/s41586-018-0546-8.

Received: 4 October 2017; Accepted: 27 July 2018;
Published online 26 September 2018.

1. Travis, B. V. et al. The more effective mosquito repellents tested at the Orlando, Fla., laboratory, 1942–47. *J. Econ. Entomol.* **42**, 686–694 (1949).
2. McCabe, E. T., Barthel, W. F., Gertler, S. I. & Hall, S. A. Insect Repellents. III. *N*, *N*-diethylamides. *J. Org. Chem.* **19**, 493–498 (1954).
3. Tawatsin, A. et al. Field evaluation of DEET, Repel Care, and three plant based essential oil repellents against mosquitoes, black flies (Diptera: Simuliidae) and land leeches (Arhynchobdellida: Haemadipsidae) in Thailand. *J. Am. Mosq. Control Assoc.* **22**, 306–313 (2006).
4. Abramson, C. I. et al. Proboscis conditioning experiments with honeybees, *Apis mellifera caucasica*, with butyric acid and DEET mixture as conditioned and unconditioned stimuli. *J. Insect Sci.* **10**, 122 (2010).
5. Carroll, J. F., Klun, J. A. & Debboun, M. Repellency of DEET and SS220 applied to skin involves olfactory sensing by two species of ticks. *Med. Vet. Entomol.* **19**, 101–106 (2005).
6. Dogan, E. B., Ayres, J. W. & Rossignol, P. A. Behavioural mode of action of DEET: inhibition of lactic acid attraction. *Med. Vet. Entomol.* **13**, 97–100 (1999).
7. Ditzen, M., Pellegrino, M. & Vosshall, L. B. Insect odorant receptors are molecular targets of the insect repellent DEET. *Science* **319**, 1838–1842 (2008).
8. Syed, Z. & Leal, W. S. Mosquitoes smell and avoid the insect repellent DEET. *Proc. Natl Acad. Sci. USA* **105**, 13598–13603 (2008).
9. Liu, C. et al. Distinct olfactory signaling mechanisms in the malaria vector mosquito *Anopheles gambiae*. *PLoS Biol.* **8**, e1000467 (2010).
10. Pellegrino, M., Steinbach, N., Stensmyr, M. C., Hansson, B. S. & Vosshall, L. B. A natural polymorphism alters odour and DEET sensitivity in an insect odorant receptor. *Nature* **478**, 511–514 (2011).
11. DeGennaro, M. et al. *orco* mutant mosquitoes lose strong preference for humans and are not repelled by volatile DEET. *Nature* **498**, 487–491 (2013).
12. Xu, P., Choo, Y. M., De La Rosa, A. & Leal, W. S. Mosquito odorant receptor for DEET and methyl jasmonate. *Proc. Natl Acad. Sci. USA* **111**, 16592–16597 (2014).
13. DeGennaro, M. The mysterious multi-modal repellency of DEET. *Fly* **9**, 45–51 (2015).
14. Bargmann, C. I. & Horvitz, H. R. Chemosensory neurons with overlapping functions direct chemotaxis to multiple chemicals in *C. elegans*. *Neuron* **7**, 729–742 (1991).
15. Cho, C. E., Brueggemann, C., L'Etoile, N. D. & Bargmann, C. I. Parallel encoding of sensory history and behavioral preference during *Caenorhabditis elegans* olfactory learning. *eLife* **5**, e14000 (2016).
16. Reeder, N. L., Ganz, P. J., Carlson, J. R. & Saunders, C. W. Isolation of a DEET-insensitive mutant of *Drosophila melanogaster* (Diptera: Drosophilidae). *J. Econ. Entomol.* **94**, 1584–1588 (2001).
17. Stanczyk, N. M., Brookfield, J. F., Ignell, R., Logan, J. G. & Field, L. M. Behavioral insensitivity to DEET in *Aedes aegypti* is a genetically determined trait residing in changes in sensillum function. *Proc. Natl Acad. Sci. USA* **107**, 8575–8580 (2010).
18. Brand, P. et al. The origin of the odorant receptor gene family in insects. *eLife* **7**, e38340 (2018).
19. Cook, D. E., Zdraljevic, S., Roberts, J. P. & Andersen, E. C. CeNDR, the *Caenorhabditis elegans* Natural Diversity Resource. *Nucleic Acids Res.* **45**, D650–D657 (2017).
20. Doroszuk, A., Snoek, L. B., Fradin, E., Riksen, J. & Kammenga, J. A genome-wide library of CB4856/N2 introgression lines of *Caenorhabditis elegans*. *Nucleic Acids Res.* **37**, e110 (2009).
21. Bargmann, C. I., Hartwieg, E. & Horvitz, H. R. Odorant-selective genes and neurons mediate olfaction in *C. elegans*. *Cell* **74**, 515–527 (1993).
22. Zaslaver, A. et al. Hierarchical sparse coding in the sensory system of *Caenorhabditis elegans*. *Proc. Natl Acad. Sci. USA* **112**, 1185–1189 (2015).
23. Jang, H. et al. Neuromodulatory state and sex specify alternative behaviors through antagonistic synaptic pathways in *C. elegans*. *Neuron* **75**, 585–592 (2012).
24. Schiavo, G. et al. Tetanus toxin is a zinc protein and its inhibition of neurotransmitter release and protease activity depend on zinc. *EMBO J.* **11**, 3577–3583 (1992).
25. Richmond, J. E., Davis, W. S. & Jorgensen, E. M. UNC-13 is required for synaptic vesicle fusion in *C. elegans*. *Nat. Neurosci.* **2**, 959–964 (1999).
26. Speese, S. et al. UNC-31 (CAPS) is required for dense-core vesicle but not synaptic vesicle exocytosis in *Caenorhabditis elegans*. *J. Neurosci.* **27**, 6150–6162 (2007).
27. Lin, J. Y., Knutsen, P. M., Muller, A., Kleinfeld, D. & Tsien, R. Y. ReaChR: a red-shifted variant of channelrhodopsin enables deep transcranial optogenetic excitation. *Nat. Neurosci.* **16**, 1499–1508 (2013).

Acknowledgements We thank M. Crickmore, K. J. Lee, A. Singhvi, N. Yapici and members of the Vosshall Laboratory for comments on the manuscript, and for experimental assistance and advice: S. Shaham and W. Wang for assistance with chemical mutagenesis; H. Jang for assistance with chemotaxis behaviour and imaging; A. Lopez-Cruz and E. Scheer for assistance with tracking; S. Levy and E. Scheer for plasmids and strains; and A. Nguyen for early analysis of mutants (with P.S.H.). This work was conducted with support from NIH (to E.J.D., F31 DC014222) and the CGC (P40 OD010440), which provided selected strains. L.B.V. is an investigator of the Howard Hughes Medical Institute.

Reviewer information *Nature* thanks E. Poivet and the other anonymous reviewer(s) for their contribution to the peer review of this work.

Author contributions E.J.D. and L.B.V. conceived the project, wrote the manuscript and produced the figures: E.J.D. performed the experiments and analyses shown in all figures, except for Figs. 3a–e, 4m–o (performed by M.D.) and Fig. 3g (performed by X.J.). L.B.D. performed HEK293T expression. C.I.B. provided guidance, experimental design advice and data interpretation. P.S.H. made the original observation that DEET interferes with chemotaxis, and performed initial genetic screens.

Competing interests The authors declare no competing interests.

Additional information
Supplementary information is available for this paper at https://doi.org/10.1038/s41586-018-0546-8.
Reprints and permissions information is available at http://www.nature.com/reprints.
Correspondence and requests for materials should be addressed to L.B.V.
Publisher's note: Springer Nature remains neutral with regard to jurisdictional claims in published maps and institutional affiliations.

METHODS

No statistical methods were used to predetermine sample size except the experiments shown in Fig. 2e and the ADL-imaging experiments in Fig. 4, for which a power calculation was performed based on pilot data performed under similar but not identical conditions. Animals were assigned randomly to different experimental conditions and locations of behavioural experiments were pseudo-randomized each day to avoid positioning biases. Inclusion and exclusion criteria were pre-established for all experiments, and plate positions were pseudo-randomized in behaviour experiments. The investigators were not blinded to allocation during experiments and outcome assessment except for population behavioural experiments, in which a subset of the data gathered was blinded at either the allocation or scoring phase. For all tracking experiments, the experimenter was blinded to genotype during any manual linking and curation.

Nematode culture and strains. *C. elegans* strains were maintained at room temperature (22–24 °C) on nematode growth medium (NGM) plates (51.3 mM NaCl, 1.7% agar, 0.25% peptone, 1 mM $CaCl_2$, 12.9 μM cholesterol, 1 mM $MgSO_4$, 25 mM KPO_4, pH 6) seeded with *E. coli* (OP50 strain) as a food source[28,29]. Bristol N2 was used as the wild-type strain. The CB4856 (Hawaiian) strain, containing WBVar02076179 (*str-217*^{HW}) (http://www.wormbase.org/db/get?name=WBVar02076179;class=variation) and Hawaiian recombinant inbred strains for chromosome V were previously generated[20]. Generation of extra-chromosomal array transgenes was carried out using standard procedures[30], and included the transgene injected at 50 ng/μl, the fluorescent co-injection marker *Pelt-2::GFP* at 5 ng/μl (with the exception of LBV004 and LBV009, which did not include a co-injection marker), and an empty vector for a total DNA concentration of 100 ng/μl. CRISPR–Cas9-mediated mutagenesis of *str-217* was performed as described, using *rol-6* as a co-CRISPR marker[31]. The resulting *str-217* mutant strain (LBV004 *str-217(ejd001)*) results in a predicted frame-shift in the first exon (indel: insertion (AAAAAAA), deletion (CTGCTCCA), final sequence GCGTCGAAAAAAAATTTCAG; insertion is underlined). The *str-217* rescue construct (*Pstr-217::str-217::SL2::GFP*) used a 1,112-nucleotide-length fragment 56 nucleotides upstream 5′ of the translation start of *str-217*.

Microscopy and image analysis. L2-adult stage hermaphrodites were mounted on 1% agarose pads with 10 mM sodium azide (CID 6331859, Sigma-Aldrich, S2002) in M9 solution (22 mM KH_2PO_4, 42 mM Na_2HPO_4, 85.6 mM NaCl, 1 μM $MgSO_4$, pH 6). Images were acquired with an Axio Observer Z1 LSM 780 with Apotome a 63× objective (Zeiss), and were processed using ImageJ.

Chemotaxis assays. Chemotaxis was tested as described[15], on square plates containing 10 ml of chemotaxis agar (1.6% agar in chemotaxis buffer: 5 mM phosphate buffer pH 6.0, 1 mM $CaCl_2$, 1 mM $MgSO_4$)[32]. Additions of either ethanol (solvent–agar) or 50% DEET (CID: 4284, Sigma-Aldrich, D100951) in ethanol (DEET–agar) were added immediately before pouring, after agar cooled to <44 °C. A total volume of 300 μl ethanol or DEET in ethanol was added to each 100 ml of agar mixture for all experiments except Figs. 1b, c, 5j, k. Plates were poured on the day of each experiment, and dried with lids off for 4 h before the start of the assay. One microlitre 1 M sodium azide was added to two spots on either side of the plate right before beginning the experiment to immobilize worms that reached the odorant or ethanol sources. Three days before all chemotaxis experiments, 4–6 L4 worms were transferred onto NGM plates seeded with *E. coli* (OP50 strain). The offspring of these 4–6 worms were then washed off of the plates and washed twice with S-Basal buffer (1 mM NaCl, 5.74 mM K_2HPO_4, 7.35 mM KH_2PO_4, 5 μg/ml cholesterol at pH 6–6.2)[28] to remove younger worms, and once with chemotaxis buffer. Immediately before the start of the experiment, two 1-μl drops of odorant diluted in ethanol, or ethanol solvent control, were spotted on each side of the plate on top of the sodium azide spots. Between 100 and 300 worms were then placed into the centre of the plate in a small bubble of liquid. The excess liquid surrounding the worms was then removed using a Kimwipe. Odorants diluted in ethanol were used in this study at these concentrations unless otherwise noted: 1:1,000 isoamyl alcohol (CID: 31260, Sigma-Aldrich, W205702), 1:1,000 butanone (CID: 6569, Sigma-Aldrich, 360473), 10 mg/μl pyrazine (CID: 9261, Sigma-Aldrich, W401501), 1:10 2-nonanone (CID: 13187, Sigma-Aldrich, W2787513). For bacterial chemotaxis assays, 20 μl of either LB medium, or OP50 bacterial suspension grown overnight and diluted in LB medium to an optical density (OD) at 600 nm of 1.0, was applied instead of or in addition to odorants. Assays were carried out for 60–90 min at room temperature (22–24 °C) between 13:00 and 20:00 Eastern Standard Time with the exception of those in Fig. 5f, which were quantified after either 55–65 min (1 h), 115–125 min (2 h), 175–185 min (3 h) or 235–245 min (4 h). Plates were scored as soon as possible, either immediately or—if a large number of plates was being scored on the same day—plates were moved to 4 °C to immobilize worms until they could be scored. The assay was quantified by counting worms that had left the origin in the centre of the plate, moving to either side of the plate (denoted '#Odorant' or '#Control') or just above or below the origin (denoted '#Other'), and calculating a chemotaxis index as (#Odorant − #Control)/(#Odorant + #Control + #Other). A trial was discarded if fewer than 50 worms or more than 250 worms contributed to the chemotaxis index and participated in the assay.

Mutant screen. About 100 wild-type (Bristol N2) L4 worms were mutagenized in M9 solution with 50 mM ethyl methanesulfonate (EMS) (CID: 6113, Sigma-Aldrich, M0880) for 4 h with rotation at room temperature. Mutagenized worms were picked to separate 9-cm NGM agar plates seeded with *E. coli* (OP50 strain) and cultivated at 20 °C. About 5,000 F2 worms were screened for DEET resistance on 20.3-cm casserole dishes (ASIN B000LNS4NQ, model number 81932OBL11). Five worms across three assays were more than ~2 cm closer to the odorant source than the rest of the worms on the plate and were defined as DEET-resistant. This phenotype was heritable in three strains, and each strain was backcrossed to OS1917 for four generations. Whole-genome sequencing[33] was used to map the mutations to regions containing transversions presumably introduced by the EMS, parental alleles of the N2 strain used for mutagenesis and missing alleles of the wild-type strain OS1917 used for backcrossing[34,35]. LBV003 mapped to a 5-Mb region on chromosome V, which was further mapped to *str-217*. LBV002 mapped to a 6.8-Mb region on chromosome V, which was further narrowed down to a likely candidate gene, *nstp-3(ejd002)*. In LBV002, *nstp-3(ejd002)* contains a T > G transversion of the 141st nucleotide in the coding sequence, which is predicted to produce a Phe48Val substitution in this predicted sugar:proton symporter. We were unable to map the DEET-resistant mutation(s) in LBV001.

***str-217* heterologous expression in mammalian tissue culture cells.** HEK293T cells were maintained using standard protocols in a Thermo Scientific FORMA Series II water-jacketed CO_2 incubator. HEK293T cells were obtained directly from Invitrogen and were not tested for mycoplasma contamination. Cells were transiently transfected with 1 μg each of pME18S plasmid expressing *GCaMP6s*, $Gq_{\alpha}15$ and *str-217* using Lipofectamine 2000 (CID: 100984821, Invitrogen, 1168019). Control cells excluded *str-217*, but were transfected with the other two plasmids. Transfected cells were seeded into 384-well plates at a density of 2×10^6 cells/ml, and incubated overnight in FluoroBrite DMEM medium (Thermo Fisher Scientific) supplemented with fetal bovine serum (Invitrogen, 10082139) at 37 °C and 5% CO_2. Cells were imaged in reading buffer (Hanks's Balanced Salt Solution (GIBCO) + 20 mM HEPES (Sigma-Aldrich)) using GFP-channel fluorescence of a Hamamatsu FDSS-6000 kinetic plate reader at The Rockefeller University High-Throughput Screening Resource Centre. DEET was prepared at 3× final concentration in reading buffer in a 384-well plate (Greiner Bio-one) from a 46% (2 M) stock solution in DMSO (Sigma-Aldrich). Plates were imaged every 1 s for 5 min. Ten microlitres of DEET solution in reading buffer or vehicle (reading buffer + DMSO) was added to each well containing cells in 20 μl of mediun, after 30 s of baseline fluorescence recording. The final concentration of vehicle DMSO was matched to the DEET additions, with a maximum DMSO concentration of 7.8%. Fluorescence was normalized to baseline, and responses were calculated as maximum ratio (maximum fluorescence level/baseline fluorescence level) (Supplementary Data).

Calcium imaging in ADL neurons. Calcium imaging and data analysis were performed as described[36], using single young adult hermaphrodites immobilized in a custom-fabricated $3 \times 3 \times 3$ mm^3 polydimethylsiloxane (PDMS) imaging chip. *GCaMP5k* was expressed in ADL neurons under control of the *sre-1* promoter[23] and was crossed into *str-217*$^{-/-}$ and the *str-217*$^{-/-}$ rescue strain. Imaging of *unc-13* and *unc-31* mutant strains was performed by crossing *ADL::GCaMP5k*-expressing worms to the *unc-13* and *unc-31* strains and selecting for fluorescent, uncoordinated worms. Worms were acclimatized to the imaging room overnight on *E. coli* (OP50 strain)-seeded plates. All stimuli were prepared the day of each experiment, and were diluted in ethanol to 1,000× the desired concentration before being further diluted 1:1,000 in S-Basal buffer. Young adult worms were paralysed briefly in (−)-tetramisole hydrochloride (CID: 27944, Sigma-Aldrich, L9756) at 1 mM for 2–5 min before transfer into the chip to paralyse body wall muscles to keep worms stationary during imaging. All worms were pre-exposed to light (470 ± 40 nm) for 100 s before recording to attenuate the light response of ADL neurons[37]. Experiments consisted of the following stimulation protocol: 20 s S-Basal buffer, followed by 3 repetitions of 20 s DEET (0.15% DEET and 0.15% ethanol in S-Basal) and then 20 s S-basal buffer. ADL-neuron responses desensitize rapidly[37], so only the first of the three DEET pulses was analysed.

All GCaMP signals were recorded with Metamorph Software (Molecular Devices) and an iXon3 DU-897 EMCCD camera (Andor) at 10 frames/s using a 40× objective on an upright Zeiss Axioskop 2 microscope. Custom ImageJ scripts[15] were used to track cells and quantify fluorescence. In Fig. 4b, f, j, all frames in 20 s before the DEET pulse were averaged and divided by the average of the frames during the 20-s DEET or C9 pulse to calculate ΔF. In Fig. 4c, g, k, traces were bleach-corrected using a custom MATLAB script and then the 5% of frames with the lowest values were averaged to create F_0. $\Delta F/F_0$ was calculated by $(F - F_0)/F_0$ and then divided by the maximum value to obtain[38] $\Delta F/F_{max}$. The average value during the stimulus was calculated for each worm and plotted as a single dot in Fig. 4d, h, l. The heat-map traces in Fig. 4c, g, k were also smoothed

by 5 frames, such that each data point (n) is the running average of $n-2$, $n-1$, n, $n+1$ and $n+2$.

Calcium imaging in AWC, ASH and AWB neurons. Calcium imaging of freely moving worms and subsequent data analysis were performed as described[38], using a 3-mm^2 microfluidic PDMS device with two arenas that enabled simultaneous imaging of two genotypes with approximately 10 worms each. For imaging in AWC neurons, we used an integrated line (CX17256) that expresses *GCaMP5a* in AWC^{ON} neurons under control of the *str-2* promoter, crossed into *str-217*$^{-/-}$ worms. Adult hermaphrodites were first paralysed for 80–100 min in 1 mM (−)-tetramisole hydrochloride and then transferred to the arenas in S-Basal buffer. The stimulus protocol was as follows: in S-Basal, three pulses of 60 s in buffer and 30 s in isoamyl alcohol, followed by 120 s in buffer. Next, the worms were switched to S-Basal with 0.15% ethanol (solvent buffer) and three pulses of 60 s in buffer and 30 s in isoamyl alcohol in solvent buffer, followed by 120 s in solvent buffer before a switch to S-Basal with 0.15% ethanol and 0.15% DEET (DEET buffer). In DEET buffer, worms were given 6 pulses of 60 s in DEET buffer and then 30 s in isoamyl alcohol in DEET buffer, followed by 120 s in DEET buffer before switching to solvent buffer. In solvent buffer, the worms received three pulses of 60 s in buffer and 30 s in isoamyl alcohol in solvent buffer, followed by 120 s in solvent buffer before a switch to S-Basal. In S-Basal, the worms received three pulses of 60 s in buffer and 30 s isoamyl alcohol, followed by 60 s in buffer.

Each experiment was repeated 3–4 times over 2–3 days and pooled by strain for analysis (wild type: 31 worms, 4 experiments, 3 days; *str-217*$^{-/-}$: 23 worms, 3 experiments, 2 days). Images were acquired at 10 frames/s at 5× magnification (Hamamatsu Orca Flash 4 sCMOS), with 10-ms pulsed illumination every 100 ms (Sola, Lumencor; 470/440-nm excitation). Fluorescence levels were analysed using a custom ImageJ script that integrates and subtracts the background fluorescence levels of the AWC neuron cell body (6 × 6 pixel region of interest). Traces were normalized by subtracting and then dividing by the baseline fluorescence, defined as the average fluorescence of the last 2 s of the first 3 isoamyl alcohol pulses. The traces in Fig. 3a, b were also smoothed by 5 frames, such that each data point (n) is the running average of $n-2$, $n-1$, n, $n+1$ and $n+2$. The response magnitudes in Fig. 3c were calculated by taking the mean of the last 2 s of an isoamyl alcohol pulse, subtracting the mean of the 2 s before the isoamyl alcohol pulse (F_0), and dividing by this F_0. The response magnitudes were calculated for the 5th (0.15% ethanol in S-Basal buffer) and 8th (0.15% DEET and 0.15% ethanol in S-Basal buffer) isoamyl alcohol pulses.

Calcium imaging in ASH neurons was performed similarly, with the following exceptions. For imaging in ASH neurons, we used a strain (CX10979) expressing *GCaMP3* in ASH neurons under control of the *sra-6* promoter. The stimulus protocol used was as follows: 60 s in S-Basal, 60 s in 0.15% ethanol in S-Basal buffer, 60 s in S-Basal, 60 s in 0.15% DEET in S-Basal and finally 60 s in S-Basal buffer. Each experiment was repeated over 2 days and pooled for analysis (wild type: 15 worms in 2 experiments on 2 different days).

Calcium imaging in AWB neurons was performed similarly to imaging in AWC neurons, with the following exceptions. For imaging in AWB neurons, we used a control strain (CX17428) expressing *GCaMP5a* in AWB neurons under the *str-1* promoter and a test strain (CX17660) expressing *GCaMP5a* under the *str-1* promoter, as well as expressing *str-217* in AWB neurons under the *str-1* promoter. Adult hermaphrodites were first similarly paralysed in 1 mM (−)-tetramisole hydrochloride for 80–100 min, but the first 65–75 min was in S-Basal buffer and the last 15 min was 1 mM (−)-tetramisole hydrochloride in ethanol–buffer. The stimulus protocol used was as follows: 60 s in 0.15% ethanol in S-Basal buffer, 10 s in 0.15% DEET and 0.15% ethanol in S-Basal buffer, and 60 s in 0.15% ethanol in S-Basal buffer. A 4 × 4-pixel region of interest was used during tracking of the neurons. Baseline fluorescence was defined as the median fluorescence of the 10 s preceding the DEET pulse. Response and peak magnitudes were calculated using traces smoothed by 5 frames and identifying the maximum value within the DEET pulse. Five sets of experiments were conducted over 3 days for a total of 41 wild-type worms and 49 worms expressing *str-217*.

In Fig. 4n, traces were bleach-corrected using a custom MATLAB script and then the 5% of frames with the lowest values were averaged to create F_0. $\Delta F/F_0$ (%) was calculated[38] by $(F - F_0)/F_0$. The heat-map traces in Fig. 4n were also smoothed by 5 frames, such that each data point (n) is the running average of $n-2$, $n-1$, n, $n+1$ and $n+2$. Peak $\Delta F/F_0$ (%) in Fig. 4o reflects the maximum value of $\Delta F/F_0$ (%) during the DEET pulse.

Chemotaxis tracking and analysis. Between 8 and 20 adult hermaphrodites were first transferred to an empty NGM plate and then 4–15 were transferred to an assay plate to minimize bacterial transfer. Worms were then placed in the centre on either a 0.15% DEET–agar or solvent–agar plate, and their movement was recorded for 60 min at 3 frames/s with 6.6 MP PL-B781F CMOS camera (PixeLINK) and Streampix software. Assays were carried out at room temperature, between 12:00 and 20:00 Eastern Time, and lit from below. Worm trajectories were extracted by a custom MATLAB (MathWorks) script[15], and discontinuous tracks were then manually linked. Tracks were discarded if the worm moved less than two body lengths from its origin over the course of the 60-min trial. If a worm came within 1 cm of the isoamyl alcohol stimulus, the track was truncated to remove information from worms immobilized at the odorant source because of the addition of sodium azide.

ADL optogenetic stimulation. L4 worms expressing an *Psrh-220::ReaChR*[27] array or array-negative worms from the same plate were raised overnight in the dark on an NGM plate freshly seeded with 100 µl of 10× concentrated *E. coli* (OP50 strain) with or without 50 µM all-*trans* retinal (CID: 720648, Sigma-Aldrich, R2500), which is required for ReaChR-induced activity. The next day, adult hermaphrodites were first transferred to an empty NGM plate and then 4–15 worms were transferred to the 10-cm circular assay plate to minimize bacterial transfer. Videos were recorded for 26 min at 3 frames/s with a 1.3 MP PL-A741 camera (PixeLINK) and Streampix software. Blue light pulses were delivered with an LED (455 nm, 45 µW/mm^2, Mightex) controlled with a custom MATLAB script[15,39]. Worms were exposed to normal light for 120 s, before exposure to 6 repetitions of blue light (10 Hz strobing) for 120 s, and 120 s of recovery (LED off). Worm trajectories were extracted by a custom MATLAB script[39]. Pausing events were extracted, and all pauses ≥ 3 frames (1 s) were used for further analysis. Pauses were classified as 'on' if any frame included light illumination. A pause that began just before illumination began—but remained paused while the illumination occurred—was considered an 'on' pause; any pauses that began during light illumination were also considered to be 'on'. All other pauses were classified as 'off' pauses. In the analysis in Fig. 5j, we took an average pause length for all on and off pauses for each worm and pooled all of the worms on each plate. To control for any baseline differences between worms and experiment-to-experiment variation, we examined the increase in average pause length in Fig. 5k.

Phylogenetic analysis of *str-217* in wild isolates. Data were obtained from CeNDR[19]. Only predicted deletions in exons or missense changes of high confidence were included (Supplementary Data).

Statistical analysis. R v.3.3.2 was used for all statistical analysis. Additionally, qqPlots were evaluated before performing ANOVAs. For the analysis of optogenetic experiments, a Levene's test identified heteroscedasticity in these data that was addressed with a boxcox translation. Imaging data from AWC neurons were similarly boxcox-translated and transformed to adjust for the rightward skew.

Strains. Detailed genotypes of all *C. elegans* strains and their sources are provided in Supplementary Data.

Reporting summary. Further information on research design is available in the Nature Research Reporting Summary linked to this paper.

Data availability

All scripts and graphed data with the exception of raw video files are available in the Supplementary Data. Raw video files are available on request from the corresponding author.

28. Brenner, S. The genetics of *Caenorhabditis elegans*. *Genetics* **77**, 71–94 (1974).
29. Stiernagle, T. in *WormBook* (ed. The *C. elegans* Research Community, WormBook) https://www.doi.org/10.1895/wormbook.1.101.1 (2006).
30. Mello, C. & Fire, A. DNA transformation. *Methods Cell Biol*. **48**, 451–482 (1995).
31. Arribere, J. A. et al. Efficient marker-free recovery of custom genetic modifications with CRISPR/Cas9 in *Caenorhabditis elegans*. *Genetics* **198**, 837–846 (2014).
32. Hart, A. C. (ed.) in *WormBook* (ed. The *C. elegans* Research Community, WormBook) https://www.doi.org/10.1895/wormbook.1.87.1 (2006).
33. Sarin, S. et al. Analysis of multiple ethyl methanesulfonate-mutagenized *Caenorhabditis elegans* strains by whole-genome sequencing. *Genetics* **185**, 417–430 (2010).
34. Zuryn, S., Le Gras, S., Jamet, K. & Jarriault, S. A strategy for direct mapping and identification of mutations by whole-genome sequencing. *Genetics* **186**, 427–430 (2010).
35. Kutscher, L. M. & Shaham, S. in *WormBook* (ed. The *C. Elegans* Research Community, WormBook) https://doi.org/10.1895/wormbook.1.167.1 (2014).
36. Larsch, J. et al. A circuit for gradient climbing in *C. elegans* chemotaxis. *Cell Rep.* **12**, 1748–1760 (2015).
37. Jang, H. et al. Dissection of neuronal gap junction circuits that regulate social behavior in *Caenorhabditis elegans*. *Proc. Natl Acad. Sci. USA* **114**, E1263–E1272 (2017).
38. Larsch, J., Ventimiglia, D., Bargmann, C. I. & Albrecht, D. R. High-throughput imaging of neuronal activity in *Caenorhabditis elegans*. *Proc. Natl Acad. Sci. USA* **110**, E4266–E4273 (2013).
39. Gordus, A., Pokala, N., Levy, S., Flavell, S. W. & Bargmann, C. I. Feedback from network states generates variability in a probabilistic olfactory circuit. *Cell* **161**, 215–227 (2015).

nature research

Corresponding author(s): Leslie B Vosshall

☐ Initial submission ☐ Revised version ☒ Final submission

Life Sciences Reporting Summary

Nature Research wishes to improve the reproducibility of the work that we publish. This form is intended for publication with all accepted life science papers and provides structure for consistency and transparency in reporting. Every life science submission will use this form; some list items might not apply to an individual manuscript, but all fields must be completed for clarity.

For further information on the points included in this form, see Reporting Life Sciences Research. For further information on Nature Research policies, including our data availability policy, see Authors & Referees and the Editorial Policy Checklist.

Experimental design

1. Sample size

Describe how sample size was determined.

Sample sizes for initial population behavior assays for commonly used odorants and DEET as a point source were chosen based on common practice. Later experiments with inbred strains and newly created strains were increased based on pilot data that showed the chemotaxis indices were more variable for Hawaiian containing lines. A power analysis was performed on these pilot data using R package 'pwr' at f=0.5, alpha=0.05, and power=0.8. We then collected greater than or equal to the minimum suggested number of observations based on this power calculation. For individual animal tracking data, all experiments were completed as described in the manuscript with a sample size (~6 data points) comparable to other similar data sets generated in the literature. This consensus was built empirically based on experience and many data sets but not formally tested. Sample size was kept consistent across all experiments. The number of animals added to each plate was determined based on the empirical observation that adding additional animals made the tracking of individuals much more difficult as the number of collision and overlap events increased. AWC imaging sample size was determined by the number of animals that could fit in the chamber and be tracked, and was repeated over multiple days. ADL imaging sample sizes were determined by collecting pilot data, although these data were collected under a slightly different stimulus regime. A power analysis was performed on these pilot data using R package 'pwr' at f=0.5, alpha=0.05, and power =0.8. We then collected greater than or equal to the minimum suggested number of observations based on this power calculation and collected a similar number of observations across genotypes and treatments. HEK293T heterologous expression sample sizes were collected based on established standards in the field.

2. Data exclusions

Describe any data exclusions.

Exclusion criteria were all pre-established. For population chemotaxis assays, if more than 250 or fewer than 50 animals contributed to the chemotaxis index the data were discarded. Such conditions arose when the experimenter inadvertently added too few or too many animals to the assay plate. Only animals of the appropriate age were counted, and any young animals were not included in these chemotaxis indices. Additionally, if the temperature in the room where behavior took place changed more than 2 degrees over the course of the experiment or if positive controls showed less than 50% average chemotaxis for that day, all results from that day were discarded. For the individual animal tracking experiments, if an animal did not move more than 2 body lengths away from its origin, it was discarded. In two cases, a younger L2 animal was inadvertently placed on the plate and went unnoticed until analysis. Data from these L2 animals were discarded from analysis. After these criteria were applied, data from the plate were discarded if fewer than 2 animal tracks remained. For ADL calcium imaging results, several criteria were used. Videos were excluded from analysis if: the signal to noise ratio was too low for the neuron to be tracked, if the cell moved out of the field of view, or if there was any dust or air caught in the chip at the end of the experiment (this cannot be seen during the experiment). All genotypes were tested on the same day and if, based on these exclusion criteria, all of a particular genotype were discarded, the whole day of imaging was discarded for all genotypes.

3. Replication

Describe whether the experimental findings were reliably reproduced.

All attempts at replicating these results have been successful.

4. Randomization

Describe how samples/organisms/participants were allocated into experimental groups.

For population behavior assays, animals from several individual group-reared food/growth plates were pooled before being split apart as evenly as possible and were randomly added onto behavior plates. For individual animal tracking experiments, animals were hand-picked onto plates. All animals tested on a given day were from the same food plate or plates (if many animals were used) and assigned randomly to behavior plates. This was done randomly except for the optogenetic ReaChR expressing reagents. Non-fluorescent animals that do not express ReaChR were picked from the same bacteria+/-retinal food plates as fluorescent animals (expressing ReaChR). These were then distributed randomly onto behavioral plates and tested simultaneously. This is to control for any differences in bacteria +/- retinal lawns. For the individual animal tracking experiments, 4 cameras could be used to track 4 different plates at once. All genotypes and treatments in any given experiment were pseudo-randomly placed to control for any potential effects of side bias. For imaging experiments, fluorescent animals expressing the GCaMP reporter strain were selected by hand chosen randomly from each plate, one at a time.

5. Blinding

Describe whether the investigators were blinded to group allocation during data collection and/or analysis.

At least one day including several replicates of each population behavioral assay was performed blinded during acquisition and scoring. The aggregate results from these days followed the same trends of unblinded data, and all were pooled for formal statistical analysis as is common practice for these types of data. The individual animal tracking experiments were handled similarly: one of the days of behavior blinded during acquisition, and the rest were not, all were pooled for statistical analysis. However, any manual linkage of tracks were completed blind to genotype and treatment and then unblinded after all videos from a given day had been analyzed. The imaging data were not blinded during acquisition, but for ADL imaging, all decisions on inclusion/exclusion were made blind except the last quality control step: determining if all experiments of any given genotype had been discarded, in which case the whole day was discarded. To make this judgment, it was necessary to determine which videos belonged to which genotypes and therefore this could not be blinded. For AWC imaging, animals were only excluded if the cell body could not be tracked for the entirety of the recording or if they were outside the field of view of the camera. This was not done blinded but very few animals were excluded from analysis.

Note: all studies involving animals and/or human research participants must disclose whether blinding and randomization were used.

6. Statistical parameters

For all figures and tables that use statistical methods, confirm that the following items are present in relevant figure legends (or in the Methods section if additional space is needed).

n/a	Confirmed
☐	☒ The exact sample size (*n*) for each experimental group/condition, given as a discrete number and unit of measurement (animals, litters, cultures, etc.)
☐	☒ A description of how samples were collected, noting whether measurements were taken from distinct samples or whether the same sample was measured repeatedly
☒	☐ A statement indicating how many times each experiment was replicated
☐	☒ The statistical test(s) used and whether they are one- or two-sided (note: only common tests should be described solely by name; more complex techniques should be described in the Methods section)
☐	☒ A description of any assumptions or corrections, such as an adjustment for multiple comparisons
☐	☒ The test results (e.g. *P* values) given as exact values whenever possible and with confidence intervals noted
☐	☒ A clear description of statistics including central tendency (e.g. median, mean) and variation (e.g. standard deviation, interquartile range)
☐	☒ Clearly defined error bars

See the web collection on statistics for biologists for further resources and guidance.

Software

Policy information about availability of computer code

7. Software

Describe the software used to analyze the data in this study.	R version 3.2, Metamorph 7.8.8.0 (64-bit), ImageJ 1.49a, Streampix Version 6, and MATLAB 2014b.

For manuscripts utilizing custom algorithms or software that are central to the paper but not yet described in the published literature, software must be made available to editors and reviewers upon request. We strongly encourage code deposition in a community repository (e.g. GitHub). *Nature Methods* guidance for providing algorithms and software for publication provides further information on this topic.

Materials and reagents

Policy information about availability of materials

8. Materials availability

Indicate whether there are restrictions on availability of unique materials or if these materials are only available for distribution by a for-profit company.	All unique materials are available upon request from the authors or will be available at the time of publication from repositories including AddGene.

9. Antibodies

Describe the antibodies used and how they were validated for use in the system under study (i.e. assay and species).	No antibodies were used.

10. Eukaryotic cell lines

a. State the source of each eukaryotic cell line used.	HEK293T cells were ordered from Invitrogen
b. Describe the method of cell line authentication used.	Cells were not authenticated
c. Report whether the cell lines were tested for mycoplasma contamination.	The cell lines were not tested for mycoplasma
d. If any of the cell lines used are listed in the database of commonly misidentified cell lines maintained by ICLAC, provide a scientific rationale for their use.	These cell lines are a commonly used reagent and proper controls were performed. Because none of our data depend on the exact identity, but rather their ability to be transfected, which we controlled for, we continued to use this line.

Animals and human research participants

Policy information about studies involving animals; when reporting animal research, follow the ARRIVE guidelines

11. Description of research animals

Provide details on animals and/or animal-derived materials used in the study.	Young adult Caenorhabditis elegans hermaphrodites primarily of the wild type N2 (Bristol) except where noted and described and listed here based on CGC-approved nomenclature: ewIR73, ewIR74, ewIR76, CB4856, LBV001, LBV002, LBV003, LBV004, LBV005, LBV006, LBV007, LBV008, LBV009, CX16616, CX12328, CX17256, OS1907.

Policy information about studies involving human research participants

12. Description of human research participants

Describe the covariate-relevant population characteristics of the human research participants.	The study did not involve human research participants.